

# Pockels-effect-based adiabatic frequency conversion in ultrahigh- $Q$ microresonators

Yannick Minet<sup>1,2,\*</sup>, Luis Reis<sup>1,\*</sup>, Jan Szabados<sup>1</sup>, Christoph S. Werner<sup>3</sup>, Hans Zappe<sup>2</sup>, Karsten Buse<sup>1,3</sup> and Ingo Breunig<sup>1,3</sup>

Adiabatic frequency conversion has some key advantages over nonlinear frequency conversion. No threshold and no phase-matching conditions need to be fulfilled. Moreover, it exhibits a conversion efficiency of 100 % down to the single-photon level. Adiabatic frequency conversion schemes in microresonators demonstrated so far suffer either from low quality factors of the employed resonators resulting in short photon lifetimes or small frequency shifts. Here, we present an adiabatic frequency conversion (AFC) scheme by employing the Pockels effect. We use a non-centrosymmetric ultrahigh- $Q$  microresonator made out of lithium niobate. Frequency shifts of more than 5 GHz are achieved by applying just 20 V to 70- $\mu\text{m}$ -thick crystal. Furthermore, we demonstrate that already with the same setup positive and a negative frequency chirps can be generated. With this method, by controlling the voltage applied to the crystal, almost arbitrary frequency shifts can be realized. The general advances in on-chip fabrication of lithium-niobate-based devices make it feasible to transfer the current apparatus onto a chip suitable for mass production.

Optical frequency conversion based on nonlinear optics in microresonators has been advanced over the last decades. Nonlinear frequency conversion is based on the nonlinear response of the material to light.<sup>1</sup> For example, frequency combs in microresonators made out of centrosymmetric materials<sup>2</sup> and tunable optical OPOs in non-centrosymmetric microresonators have been demonstrated.<sup>3,4</sup> High conversion efficiencies require high intensities, as well as phase matching conditions need to be fulfilled.<sup>5</sup> Moreover, a pump threshold must be overcome for the most versatile conversion mechanism, optical parametric oscillation. An alternative optical conversion technique is the so-called adiabatic frequency conversion (AFC). Here, the frequency of light traveling in a resonator is shifted due to a change of the optical round-path length. One implementation is to change the refractive index of the material and to keep the geometrical path length constant. The frequency of light changes then accordingly to<sup>6</sup>

$$\frac{\Delta\nu}{\nu} \approx -\frac{\Delta n}{n}. \quad (1)$$

The change of the refractive index must happen in a time  $\Delta t$  shorter than the propagation time  $t$  of the light in the material, i.e. before it gets lost by absorption or scattering. Since microresonators act as light traps, that can store light for many nanoseconds or even milliseconds, depending

on their quality factor. Thus they are supposed to be well suited to realize AFC.<sup>7</sup> For AFC, no threshold has to be overcome. This frequency conversion scheme has been realized experimentally in several implementations, even down to a single photon level.<sup>8,9</sup> For example AFC was shown in photonic crystals,<sup>10–12</sup> in waveguides<sup>9,13–15</sup> and in fiber grating cavities.<sup>16</sup> So far, two different attempts involve microresonators: Conduction-band electrons generated by laser pulses, inducing a change of the refractive index allow to shift a few hundred GHz to shorter wavelengths.<sup>17</sup> However, the quality factor suffers from the generated free electrons and hence losses increase. Typical  $Q$  values are around  $10^4$ , only. Moreover the repetition rate is limited by the time it takes for the free electrons to recombine. An alternative method is to shift the frequency adiabatically to longer wavelengths via the AC-Kerr effect.<sup>18</sup> Here, a second pump laser is needed. Without affecting the quality factor being as high as  $Q = 10^7$ , frequency shifts of hundreds of megahertz can be observed. Thus these approaches come either with low  $Q$ -factors and large tuning ranges or high- $Q$  and relatively small tuning range.

Here we demonstrate adiabatic frequency conversion by employing the Pockels effect in high- $Q$  non-centrosymmetric microresonators. In contrast to the carrier-induced method we can take advantage of a linear

\*These authors contributed equally to this work.

<sup>1</sup>Department of Microsystems Engineering - IMTEK, University of Freiburg, Georges-Köhler-Allee 102, 79110 Freiburg, Germany.

<sup>2</sup>Gisela and Erwin Sick Chair of Micro-Optics, Department of Microsystems Engineering - IMTEK, University of Freiburg, Georges-Köhler-Allee 102, 79110 Freiburg, Germany.

<sup>3</sup>Fraunhofer Institute for Physical Measurement Techniques IPM, Heidenhofstraße 8, 79110 Freiburg, Germany.

dependence of the tuning on the applied electric field. The Pockels effect gives the opportunity to create both positive and negative frequency shifts, which is also not possible with approaches demonstrated so far. This allows us to create arbitrary wavelength-vs.-time functions, since the electric signal is transferred directly into a wavelength change. The resonators used in this work are fabricated out of a 300  $\mu\text{m}$ -thick wafer of  $z$ -cut 5-%-MgO-doped congruent lithium niobate (CLN). Both sides of the wafer are covered with a 150 nm-layer of chromium. First we cut out a resonator blank using frequency-doubled 388 nm femtosecond laser puls with a repetition rate of 2 kHz and an average output power of approximately 300 mW. Afterwards, the resonator blank is soldered on a brass post and then turned to a sphere using a computer-controlled laser-lathe with the same fs-laser. Finally, we polish the resonator with a diamond slurry until the intrinsic  $Q$ -factor exceeds  $Q > 10^8$ , which is limited only by the material absorption.<sup>19</sup> For the presented we fabricated two different WGRs. One resonator has a major radius of  $R = 1.2$  mm, a minor radius of  $\rho = 380$   $\mu\text{m}$  and 300  $\mu\text{m}$  thickness. To achieve larger tuning for a given voltage, we fabricated a second resonator out of a wafer lapped down to  $d = 70$   $\mu\text{m}$ . It possesses a major radius of  $R = 1$  mm and a minor radius of  $\rho = 600$   $\mu\text{m}$ . Our setup is illustrated in Fig. 1.

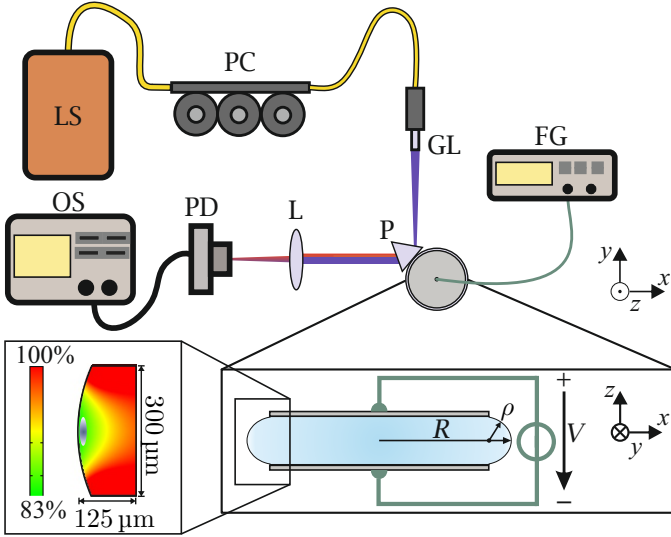


**Figure 1:** Schematic of the measurement setup. Abbreviations: Tunable laser (LS); polarization controller (PC); GRIN lens (GL); function generator (FG); lens (L); prism (P); photodiode (PD); oscilloscope (OS). The close up shows the finite element simulation of the electric field  $E_z$  in the resonator using our real geometries. The small blue area represents the volume and position of fundamental resonator mode. Here  $R$  and  $\rho$  are the major and the minor radius of the resonator.

As light sources, we use either a grating-stabilized diode laser emitting at around 1040 nm wavelength, a Ti:sapphire laser emitting light between 700-950 nm wavelength or a

telecom laser at 1.57  $\mu\text{m}$ . The laser light is then coupled into a fiber with a polarization controller. This light leaving the fiber via a gradient index lens is focused into the prism. Hence, an evanescent light field is generated on the base of the rutile prism. In order to change the coupling strength we can adjust the gap between the prism and the resonator with a piezo actuator. To generate a sufficient signal level on the detector, we couple several 100  $\mu\text{W}$  of the pump laser light into the resonator. The top and bottom of the chromium-coated resonator are electrically connected to an arbitrary-function generator providing 20 V maximum output voltage with less than 10 ns rise and fall time. The shifted light is coupled out via the rutile prism and superimposed with the pump light that is not coupled in and reflected on the prism base. These two collinear waves are focused on a photodetector that is connected to a 12.5-GHz-oscilloscope. The whole setup is placed in a box made of acrylic glass providing a temperature stabilization of 1 mK.

As illustrated in Fig. 1, the fundamental resonator mode is not between the electrodes of the resonator. Consequently, we cannot assume a simple plate capacitor model. As we move outside the edges of the electrodes of the resonator, the electric field gets weaker. For a smaller minor radius, the rim will protrude further outside the edges of the electrodes, reducing the effective electric field strength at the rim where the modes travel. By simulating the electric field  $E_z$ , we can determine the strength of the electric field at the position of the fundamental resonator mode, see Fig. 1, close up. For the thick resonator the field is reduced by a factor  $\alpha_1 = 0.83$ , and for the thin resonator with  $d_z = 70$   $\mu\text{m}$  and a larger minor radius  $\rho$  by the factor  $\alpha_2 = 0.97$ . Thus, when we apply 1 V<sub>pp</sub> the electric field is assumed to be  $E_{\text{eff},1} = E_z \alpha_1 = 2.8$  V/mm and to be  $E_{\text{eff},2} = E_z \alpha_2 = 13.9$  V/mm.

The basic principle of the Pockels-effect-based AFC is illustrated in Fig. 2. When we apply a voltage  $U$  on the electrodes of the resonator, we generate an electric field  $E_z$ . Due to the Pockels effect, the refractive index  $n$  is hence changed according to

$$\Delta n = -\frac{1}{2} n_0^3 r_\gamma E_z, \quad (2)$$

where  $\gamma \in \{33, 13\}$  indicates the different electro-optic coefficients for extraordinarily and for ordinarily polarized light. This results in a shift of the eigenfrequency of the WGR  $\nu_{\text{WGR}}(E_z)$  according to Eq. 1. The voltage applied to the electrodes leads to an electric field component  $E_z$  along the  $z$ -axis. The electro-optic coefficients for 5-%-MgO-CLN have not been determined so far. Thus, for comparison purposes, we use values for undoped CLN which are  $r_{13} \approx 8.1$  pm/V and  $r_{33} \approx 24.6$  pm/V.<sup>20</sup>

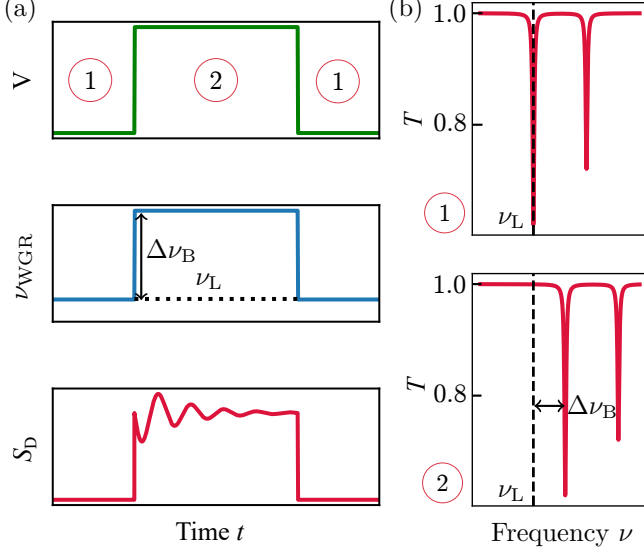


**Figure 2:** (a) By applying a square-function electrical signal, the out-coupled light changes its frequency  $\nu_{\text{WGR}}$ , while the laser frequency  $\nu_L$  stays constant. The signal  $S_D$  on the photodiode, shows an exponentially decaying oscillation. The rise/drop of the base level  $S_D$  when the voltage is switched on/off stems from the fact that with the voltage applied less pump light is coupled into the resonator and hence reflected. Thus the light power reaching the photodiode is increased. (b) Transmission spectrum of the WGR. In (1), the situation with no electric field applied and laser is coupled into a resonator mode is shown. In (2) an electric field is applied, and due to Pockels-effect-induced change of the eigenfrequency  $\Delta\nu_B$ , no light is coupled into the resonator anymore.

Due to the field-induced change of the eigenfrequency  $\nu_{\text{WGR}}$ , the laser light of frequency  $\nu_L$  is not coupled in the resonator anymore. If the shift of the resonator eigenfrequency happens faster than the decay time  $\tau$  of the resonator, the trapped light is forced to follow this change. On the photodiode we then expect to observe a beat signal  $S_D(t)$  between the out-coupled light and the original pump laser light. The signal is supposed to be described by

$$S_D(t) = I_L + I_{\text{WGR}} \exp\left(-\frac{2t}{\tau}\right) + 2\sqrt{I_L I_{\text{WGR}}} \cos(2\pi \times \Delta\nu_B t + \phi_0) \exp\left(-\frac{t}{\tau}\right). \quad (3)$$

Here  $I_L$  is the intensity of the pump laser that is reflected at the prism base,  $I_{\text{WGR}}$  is the intensity of the light leaving the WGR via the coupling prism and  $\phi_0$  is the relative phase between the out-coupled light and the laser light. The beat note has the frequency  $\Delta\nu_B = |\nu_L - \nu_{\text{WGR}}|$ , with  $\nu_L$  being the frequency of the laser light coupled into the resonator and  $\nu_{\text{WGR}}$  the frequency of the manipulated light leaving the WGR. First, we measure the beat note when we apply a periodic square signal with a frequency of 10 kHz

and an on-time of 500 ns with an amplitude of  $1 V_{\text{pp}}$  to the resonator. The signal measured by the photodiode as well as a fit of Eq. 3 to the data is shown in Fig. 3.

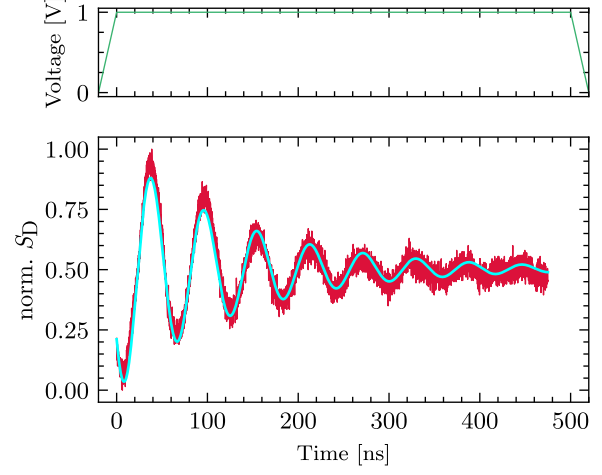


**Figure 3:** Applying a square electrical signal (green) of 1 V amplitude to the electrodes leads to a frequency shift of  $\Delta\nu_B = 17.0(1)$  MHz for o-polarized light. The decay time is determined to be  $\tau = 133$  ns (red: data, cyan: fit of Eq. 3).

We determined a decay time of  $\tau = 133$  ns. From that, we derive the quality factor  $Q = 2.4 \times 10^8$  according to  $Q = 2\pi\nu_L\tau$ . Compared with the quality factor of the resonator used in Kerr-effect-based AFC,<sup>18</sup> this is more than an order of magnitude higher. We obtain a beat frequency of  $\nu_B = 17.0(1)$  MHz. To calculate the expected value for  $\nu_B$ , we replace  $\Delta n$  in Eq. 2 by  $\Delta\nu = -\nu_L(\Delta n/n)$  from Eq. 1 and obtain

$$\Delta\nu_B = \frac{1}{2}\nu_L n^2 r E_{\text{eff}}. \quad (4)$$

For the effective electric field and  $r_{13} \approx 8.1$  pm/V we obtain  $\nu_{B,\text{theo}} = 16.1$  MHz.

In order to accomplish a larger tuning with the same voltage supply we use a thin resonator with  $d = 70$   $\mu\text{m}$ . We repeated the same measurement procedure as presented before for different voltages, wavelengths and polarizations. The resulting frequency shift are plotted in Fig. 4.

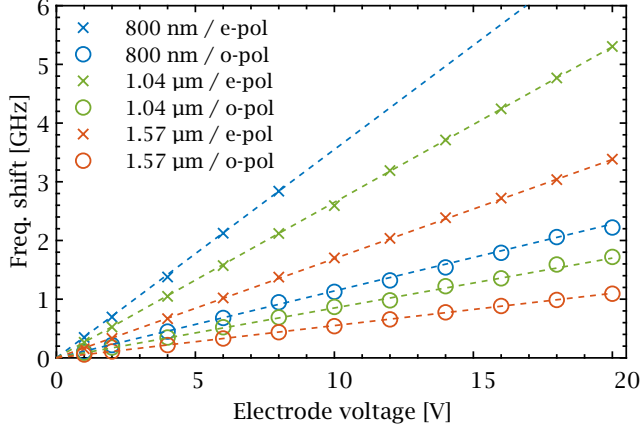


**Figure 4:** Experimental results for the obtained tuning for different light polarizations and for different applied voltages (resonator thickness  $70\text{ }\mu\text{m}$ ). The slope for e-pol. light is three times larger than that for o-pol. light due to different electro-optic coefficients  $r_{33} \approx 3 \times r_{13}$ .

Our experimental observation agrees with the expected linear behavior. Using a linear fit we determine the frequency shift per Volt, which is for light of the wavelength  $\lambda_L = 1040\text{ nm}$  either  $266(1)\text{ MHz/V}$  (e-pol.) or  $86(1)\text{ MHz/V}$  (o-pol.) To compare this result with the theoretical value we calculate the frequency shift per Volt with Eq. 4 for the effective electric field again, by employing the  $r$ -coefficients for undoped CLN.. We obtain for e-pol. light  $226.7\text{ MHz/V}$  and for o-pol. light  $80.5\text{ MHz/V}$ . This measurement and the previous one suggest that the  $r$ -coefficient is higher than assumed. For the e-pol. laser light at the wavelength  $\lambda_L = 800\text{ nm}$  we observe a slope of  $357(2)\text{ MHz/V}$ , which is almost twice the shift at  $\lambda_L = 1570\text{ nm}$ ,  $168.8(3)\text{ MHz/V}$ . The same ratio holds for the orthogonal polarization. Here the two values are  $112(1)\text{ MHz/V}$  and  $54.9(1)\text{ MHz/V}$ . This also agrees with our expectations. Neglecting small differences for the refractive index  $n$  and the electro-optic coefficient  $r$  at these two different wavelengths, we obtain twice the frequency shift by doubling of the laser frequency (Eq. 4). So far, we used a square electrical signal form only. We studied also the influence of a triangular electrical signal applied to the electrodes of the  $300\text{-}\mu\text{m}$ -thick resonator with a frequency of  $10\text{ kHz}$  and  $50\text{ ns}$  of on-time. Since the electric field is changing its strength linearly with time, the frequency of the out-coupled light shifts linearly as well. The frequency chirp and the electric signal are shown in Fig. 5. At the beginning and the end of the triangular electric signal, a beat frequency  $\Delta\nu_B \approx 0.2\text{ GHz}$  is observed. The maximum frequency  $\Delta\nu_B \approx 1\text{ GHz}$  is reached at the maximum voltage of  $20\text{ V}$ . After reaching this, we obtain a negative frequency chirp for the negative side of the triangular signal.

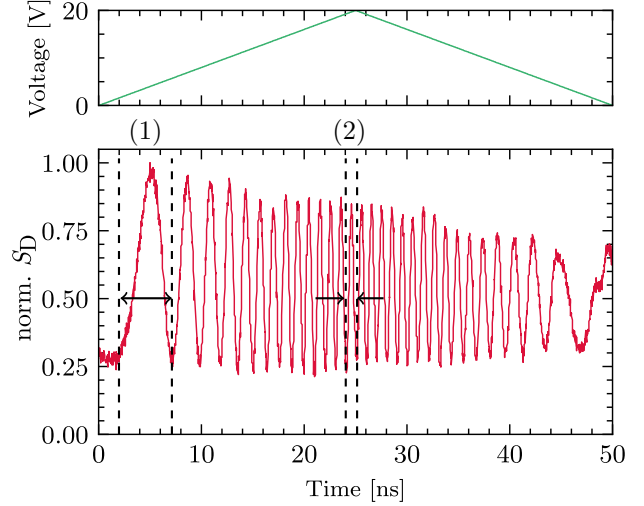


**Figure 5:** Applying a triangular electrical signal (green) to the electrodes of the resonator with  $d = 300\text{ }\mu\text{m}$  leads to a positive frequency chirp and once the maximum voltage has been passed, a negative one, in this case shown for e-polarized light out-coupled from the resonator. In (1) we measured a period length of  $\Delta t_1 \approx 5\text{ ns}$  and in (2) a period length  $\Delta t_2 \approx 1\text{ ns}$ . This corresponds to beat frequencies  $\Delta\nu_{B1} = 0.2\text{ GHz}$  and  $\Delta\nu_{B2} = 1\text{ GHz}$ , respectively.

To conclude, we demonstrated adiabatic frequency conversion in a high- $Q$  microresonator made out of lithium niobate by employing the Pockels effect. We showed more than  $5\text{ GHz}$  tuning for e-polarized light and more than  $2\text{ GHz}$  for o-polarized light. We have realized AFC for different wavelengths. Moreover, positive and negative frequency chirps have been demonstrated. In contrast to other AFC schemes in microresonators shown so far, Pockels-effect-based AFC enables large tuning by maintaining a high quality factor resulting in a long decay time. Furthermore, our setup is technically less challenging: The tuning range is limited only by the maximum output voltage of the function generator. It has been shown that lithium niobate can withstand strong electric fields of up to  $65\text{ kV/mm}$ ,<sup>21</sup> corresponding to a refractive index  $\Delta n$  of  $4.8 \times 10^{-3}$  for o-polarized light. Such a refractive index change would lead to frequency shifts of a few THz.

The presented method was realized with bulk lithium niobate whispering-gallery resonators. Despite this approach, a transfer to batch-processed chip-integrated resonators is feasible as we judge from recent advances of this technology platform.<sup>22,23</sup> Thinner resonators with lithium-niobate-on-insulator providing a  $d$  of only  $2\text{ }\mu\text{m}$  allow tuning over tens of GHz with considerably lower voltage. Many applications can be envisaged. Just as one example, AFC is a possible candidate to serve for frequency modulated continuous wave LIDAR systems.

# Acknowledgments

The authors thank S.J. Herr for his valuable contributions in the early stage of the presented work and B. Aatz, D.

Rutsch and F. Thielemann for technical support.

- <sup>1</sup> R. W. Boyd, *Nonlinear optics* (Academic Press, 2008), 3rd ed.
- <sup>2</sup> T. Herr, V. Brasch, J. D. Jost, C. Y. Wang, N. M. Kondratiev, M. L. Gorodetsky, and T. J. Kippenberg, *Nature Photonics* **8**, 145 (2014).
- <sup>3</sup> J. U. Fürst, D. V. Strekalov, D. Elser, A. Aiello, U. L. Andersen, C. Marquardt, and G. Leuchs, *Physical Review Letters* **105**, 263904 (2010).
- <sup>4</sup> I. Breunig, *Laser & Photonics Reviews* **10**, 569 (2016).
- <sup>5</sup> M. Ebrahim-Zadeh, Continuous-wave optical parametric oscillators, in *Optical properties of materials, Nonlinear Optics, Quantum Optics*, , vol. 4 of *Handbook of Optics* M. Bass, ed. (McGraw-Hill, 2010), p. 17.1.
- <sup>6</sup> M. Notomi and S. Mitsugi, *Phys. Rev. A* **73**, 051803 (2006).
- <sup>7</sup> A. A. Savchenkov, A. B. Matsko, V. S. Ilchenko, and L. Maleki, *Optics Express* **15**, 6768 (2007).
- <sup>8</sup> S. Preble, L. Cao, A. Elshaari, A. Aboketaf, and D. Adams, *Applied Physics Letters* **101**, 6 (2012).
- <sup>9</sup> L. Fan, C.-L. Zou, M. Poot, R. Cheng, X. Guo, X. Han, and H. X. Tang, *Nature Photonics* **10**, 766 (2016).
- <sup>10</sup> T. Tanabe, E. Kuramochi, H. Taniyama, and M. Notomi, *Opt. Lett.* **35**, 3895 (2010).
- <sup>11</sup> T. Tanabe, M. Notomi, H. Taniyama, and E. Kuramochi, *Physical Review Letters* **102**, 043907 (2009).
- <sup>12</sup> K. Kondo and T. Baba, *Phys. Rev. A* **97**, 033818 (2018).
- <sup>13</sup> T. Kampfrath, D. M. Beggs, T. P. White, A. Melloni, T. F. Krauss, and L. Kuipers, *Phys. Rev. A* **81**, 043837 (2010).
- <sup>14</sup> J. Upham, Y. Tanaka, T. Asano, and S. Noda, *Applied Physics Express* **3**, 062001 (2010).
- <sup>15</sup> K. Kondo and T. Baba, *Physical Review Letters* **112**, 223904 (2014).
- <sup>16</sup> I. V. Kabakova, Z. Yu, D. Halliwell, P.-Y. Fonjallaz, O. Tarasenko, C. M. de Sterke, and W. Margulis, *Journal of the Optical Society of America B* **29**, 155 (2012).
- <sup>17</sup> S. F. Preble, Q. Xu, and M. Lipson, *Nature Photonics* **1**, 293 (2007).
- <sup>18</sup> W. Yoshiki, Y. Honda, M. Kobayashi, T. Tetsumoto, and T. Tanabe, *Optics Letters* **41**, 5482 (2016).
- <sup>19</sup> M. Leidinger, S. Fieberg, N. Waasem, F. Kühnemann, K. Buse, and I. Breunig, *Optics Express* **23**, 21690 (2015).
- <sup>20</sup> A. Méndez, A. García-Cabañes, E. Diéguez, and J. M. Cabrera, *Electronics Letters* **35**, 498 (1999).
- <sup>21</sup> M. Luennemann, U. Hartwig, G. Panotopoulos, and K. Buse, *Applied Physics B* **76**, 403 (2003).
- <sup>22</sup> R. Wolf, I. Breunig, H. Zappe, and K. Buse, *Optics Express* **25**, 29927 (2017).
- <sup>23</sup> C. Wang, M. Zhang, X. Chen, M. Bertrand, A. Shams-Ansari, S. Chandrasekhar, P. Winzer, and M. Lončar, *Nature* **562**, 101 (2018).